AIMS Materials Science, 4(3): 789-799.
DOI: 10.3934/matersci.2017.3.789
Received: 07 March 2017
Accepted: 08 June 2017
Published: 16 June 2017

http://www.aimspress.com/journal/Materials

Research article

Optimization of active-layer thickness, top electrode and annealing temperature for polymeric solar cells

Said Karim Shah [1,*], Jahangeer Khan [2], Irfan Ullah [1], and Yaqoob Khan [3]

[1] Department of Physics, Abdul Wali Khan University, Mardan 23200, Khyber Pukhtunkhwa, Pakistan
[2] Wuhan National Laboratory for Optoelectronics, Huazhong University of Science and Technology, China
[3] National Centre for Physics, 44000, Islamabad, Pakistan

* **Correspondence:** Email: saidkarim@awkum.edu.pk.

Abstract: Organic solar cells, processed from solution at various optimizing device parameters, were investigated. The device's active-layer film-thicknesses were optimized while depositing at different spin speeds where 120-nm-thick layer (D2) gives maximum power conversion efficiency of 2.9%, annealed at 165 °C. The reason is ascribed as sufficient light absorption, excitons dissociation/diffusion and carriers transportation. In the case of Ca/Al, being as a top electrode rather than LiF/Al and Al, substantial efficiency enhancement, from 1.70% to 2.78%, was obtained at low temperature, 130 °C, providing ease for charge collection and pertaining conductive nature of increased resistivity at high temperature.

Keywords: polymeric solar cells; solution processed; spin coating; active-layer thicknesses; top-metal electrodes; thermal annealing

1. Introduction

Organic solar cell devices, processed from solution at room temperature, have been attracting great attention of scientific communities during the past decades owing to their low materials cost, mechanically flexible, easy fabrication over large-area substrates. The most common structure of such devices consists of donor and acceptor phases. These phases contain the electron donor and hole transporting materials, such as poly (3-hexylthiophene) (P3HT), and an electron acceptor and

transporting materials, such as (6,6)-phenyl C_{61} butyric acid methyl ester (PCBM). The acceptor and donor materials were blended together to form bulk films [1,2,3] for the devices, called bulk heterojunction organic solar cells, and have been widely investigated [4–11]. The bulk-heterojunction-solar-cell-devices concept led to enhance the short-circuit current of organic solar cell and resulting higher-power-conversion (PCE) efficiency up to 10% [12–15]. Active-layer film-thickness is a critical component of the organic solar cells devices. Tuning the device's active-layer thickness, is a point of worth noting to get optimum optical absorption, increasing charge carriers transport, and hence enhancing power conversion efficiency [16,17]. However, the active-layer thickness must be comparable to the excitons diffusion/dissociation range to suppress internal as well as contact resistances and get efficient device controlling parameters [18]. Different active-layer thicknesses have been selected in between electrodes to achieve high-light harvesting rate [4]. Kirchartz et al. observed that the variation in short circuit current density (J_{SC}) and fill factor (FF) with film thicknesses are due to the mobility and lifetime before recombination or decay, of the charge carriers [19]. Few attempts have been made on addressing the improvement of device efficiency through materials and metal electrode optimization with different light trapping strategies [20,21,22]. Various composition layers have been incorporated in between electrode and photoactive materials [23–26]. The insertion of thin layer of LiF or Ca before Al metal electrode deposition is to reduce the interfacial resistance and prevent quenching of excitons due to particular interaction at the interface [27,28]. It is also crucial to enhance the fill factor (FF) significantly and maintain high-open-circuit voltages (V_{oc}) of the devices with optimum value of temperature [29]. Thermal annealing improves absorption coefficient due to film morphology, facilitates the phase separation, thereby enhances crystallinity, increases excitons-generation rates and strengthens electrical polarizations in the P3HT:PCBM blend [7,8,30]. Thermal treatment of the P3HT/PCBM-based organic photovoltaic OPV devices is to recover the order structure of P3HT that is disrupted in the presence of PCBM during bulk film fabrication and, more interestingly, also increase the P3HT molecule chains π–π overlapping [9,12,13,31,32]. Thermal annealing on the blend films (P3HT/PCBM) plays an important role in the OPV device application. It can help to reduce series resistance of the device as well as improve the interfacial contacts between the electrodes [16,32]. Despite the various advantages over its conventional inorganic counterparts, organic solar cells have some limitations like low-charge-carrier mobility and short exciton life time [33,34,35]. Among the variety of device's active-layer-deposition techniques, spin coating, beside some limitations, is quite fast, easy and quite common to fabricate solution-processed active-layers thin and homogeneous films for optoelectronic devices [33]. A prerequisite for getting the high efficiency is optimizing the device-fabricating parameters, such as active layer thickness, post deposition annealing and cathode material layer etc. Donor and acceptor layer should have optimum thickness to harvest sufficient light and obtain efficient charge-carrier generation. Furthermore, the electrode materials are required to have an efficient charge-carrier extraction and low or non-resistive transportation. Hereby, the thickness of the donor and acceptor material, thermal annealing and inter-layer, sandwiched between top electrode and active layer, are important device parameters.

In this paper, we focus on optimization of various parameters based on P3HT:PCBM blend active layers. To this aim, optimization of the device active-layers thicknesses, top electrodes and the effect of post-thermal treatment were investigated. Initially, we deposited device's bulk layer from optimum solution concentration in order to address thickness effect. Secondly, three set of devices with different schemes of top electrode, such as Al, LiF/Al, and Ca/Al, were used. The electrical

characterization is carried out to measure the effect of thermal annealing on short-circuit current, open circuit voltage, fill factor and power conversion efficiency at different active-layer thicknesses and different top electrodes.

2. Materials and Method

In this work, the spin coating process was used to prepare the active layers for organic solar cells. Commercially available P3HT (Plextronics) and $PC_{61}BM$ (Solaris) were used without further purification. Indium-tin-oxide (ITO) substrates, with 15 Ω/cm^2 sheet resistance, were used as transparent conducting electrode. ITOs were cleaned in successive solutions of acetone, ethanol and isopropanol respectively. The substrates were sonicated for 15 minutes in each solvent. The transparent hole-conducting-polymer film around 30 nm, poly(3,4-ethylenedioxythiophene):polystyrene sulfonate (PEDOT:PSS) (Aldrich) was subsequently spin-coated from water solution on ITO/glass substrates at 4000 rpm for 40 seconds. The films were, then, annealed at 110 °C for 30 minutes. Device's active layers were prepared from the 40 mg/ml blend-concentrated solution (P3HT/PCBM) (1:1 w/w), dissolved in dichlorobenzene, using various spin-coating speed in the range of 2000 rpm to 5000 rpm under N_2 atmosphere. Thicknesses of active layers of devices were confirmed, using KLA-Tencor Alpha step 500 profilometer, to be 230 nm, 180 nm, 120 nm and 90 nm, and labeled as D4, D3, D2 and D1, respectively, for simplicity. Top metal electrodes with a scheme, such as Al, LiF/Al and Ca/Al, were evaporated through electron beam. UV-vis spectra of thin film of various devices in term of thicknesses were recorded over the spectral range of 300–800 nm using spectrometer (Perken Elmer λ 25). A 100-nm thick aluminum electrode was thermally deposited by electron-beam-evaporation process at a base pressure of 5×10^{-7} mbar onto the active layer using shadow mask to define an active-device area of 10 mm^2 to complete the devices. Fabricated organic-bulk-heterojunction solar cells with Al and thin layer (20 nm) of LiF/Ca Al, evaporated via e-beam evaporation, are shown in Figure 1a and 1b, respectively. Current-density-voltage (J-V) characteristics of devices were examined under solar simulated AM1.5G irradiation (100 $mW \cdot cm^{-2}$) using a Keithley (2400 source measuring unit a reference Si solar cell).

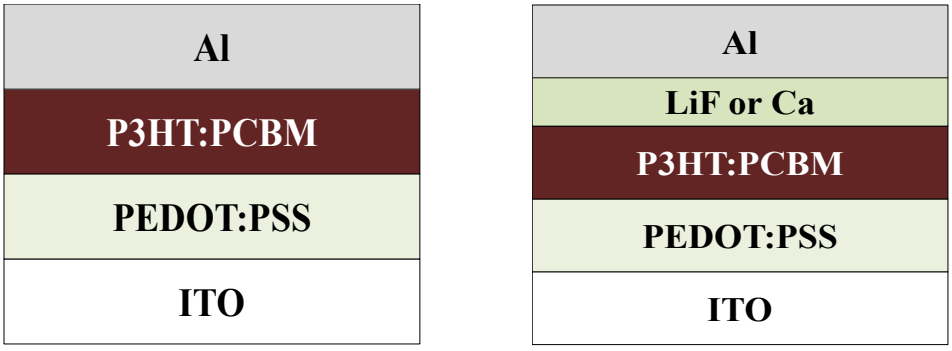

Figure 1. Fabricated bulk-heterojunction polymeric solar cells with different top electrodes: (a) Al and (b) Al/LiF or Al/Ca.

3. Results and Discussion

To improve the light absorption, active material with varying thicknesses has been introduced. Optical absorbance spectra were measured which infer clearly the thickness effect on the photon absorption, indicated in Figure 2. Absorption of films at visible range of 400–580 nm decreased significantly with decreasing thickness. A descending trend in the absorption is clearly viewed while going from the thicker, 230 nm (black), to thinner, 90 nm (dark green), film. The observations recorded indicate efficient-photon absorption by increasing the number density and hence generating charge carriers. Shoulder peaks around 600 nm were observed for all spectra that indicates well-ordered structure of P3HT molecules [36,37].

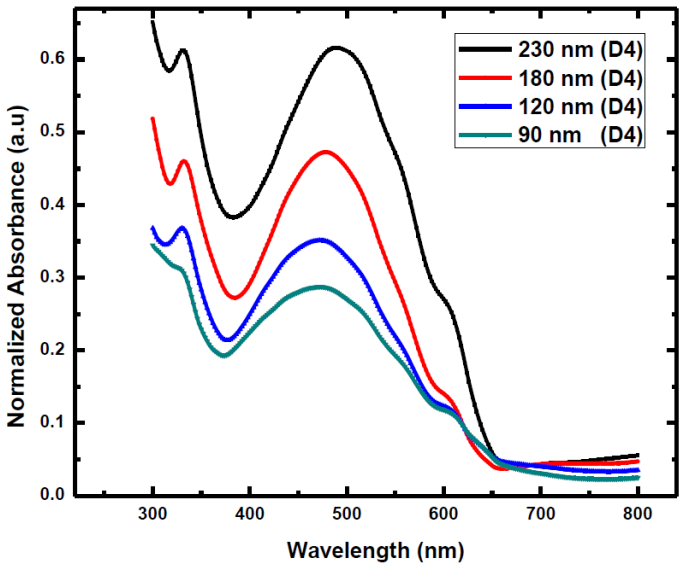

Figure 2. UV-vis absorbance spectra of the P3HT:PCBM blend with different thicknesses: 230 nm (black), 180 nm (red), 120 nm (blue) and 90 nm (green).

Figure 3 shows current-density-voltage characteristics of the organic phtovoltaics (OPVs) with optimum annealing temperature of 165 °C. It is observed that there is not much difference in the open-circuit voltage of the OPVs while changing the thickness of devices, whereas short-circuit current-density gradually increases to the optimum thickness, due to stronger built-in electric field which results in shorter pathways for charge carriers to their respective electrodes. Also increase in J_{SC}, upon high annealing temperature, shows a thermally excited hopping in these disordered systems [38]. The probability of exciton recombination is relatively high in the thicker films. Therefore, the device D2 (120-nm thick and fabricated with 4000-rpm spin-coating speed) shows an enhanced performance compared to the rest of the three devices. The enhanced device parameters, such as short-circuit current density, open-circuit voltage fill factor, and power-conversion efficiency were obtained at annealing temperature of 165 °C, as reported in Table 1. Low series resistance of 9 ohms and high shunt resistance of 1027 ohms, showing good diode behavior with high rectification and high fill factor, suggest less recombination effect.

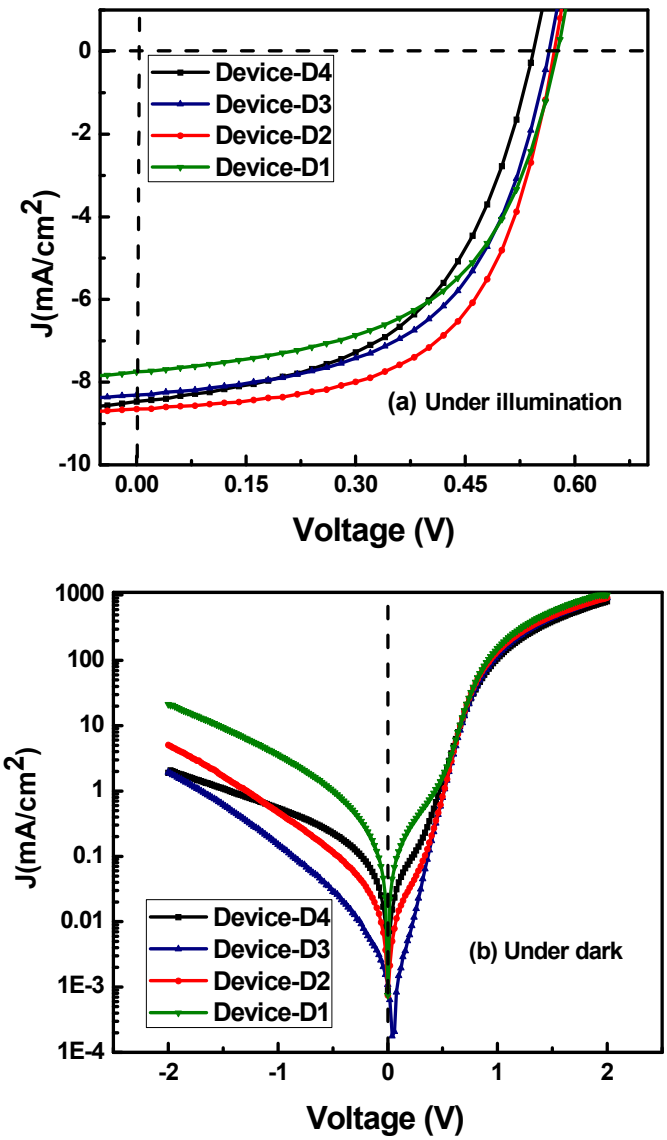

Figure 3. J-V characteristic curves of the fabricated devices with different thicknesses at optimized annealed temperature of 165 °C having Al as top electrode: under (a) illumination and (b) dark.

Table 1. Summary of OPVs parameters, J_{sc}, V_{oc}, FF, and PCE, of devices with different thicknesses at optimized annealed temperature of 165 °C having Al as top electrode.

Devices	J_{sc} (mA/cm^2)	V_{oc} (V)	FF (%)	PCE (%)
D4	8.4	0.54	53	2.4
D3	8.5	0.58	53	2.6
D2	8.7	0.58	58	2.9
D1	7.7	0.58	54	2.4

The thermal annealing effect was observed by plotting device parameters versus annealing temperature varying from 100 °C to 170 °C as illustrated in Figure 4. The more is the annealing

temperature of devices, the higher is their performance within the range of optimum value of annealing temperature. It was also noted that thermal treatment increases the power-conversion efficiency, probably due to the improvement in interfacial contacts, within the optimum value of active-layer thicknesses, hence reducing the series resistance.

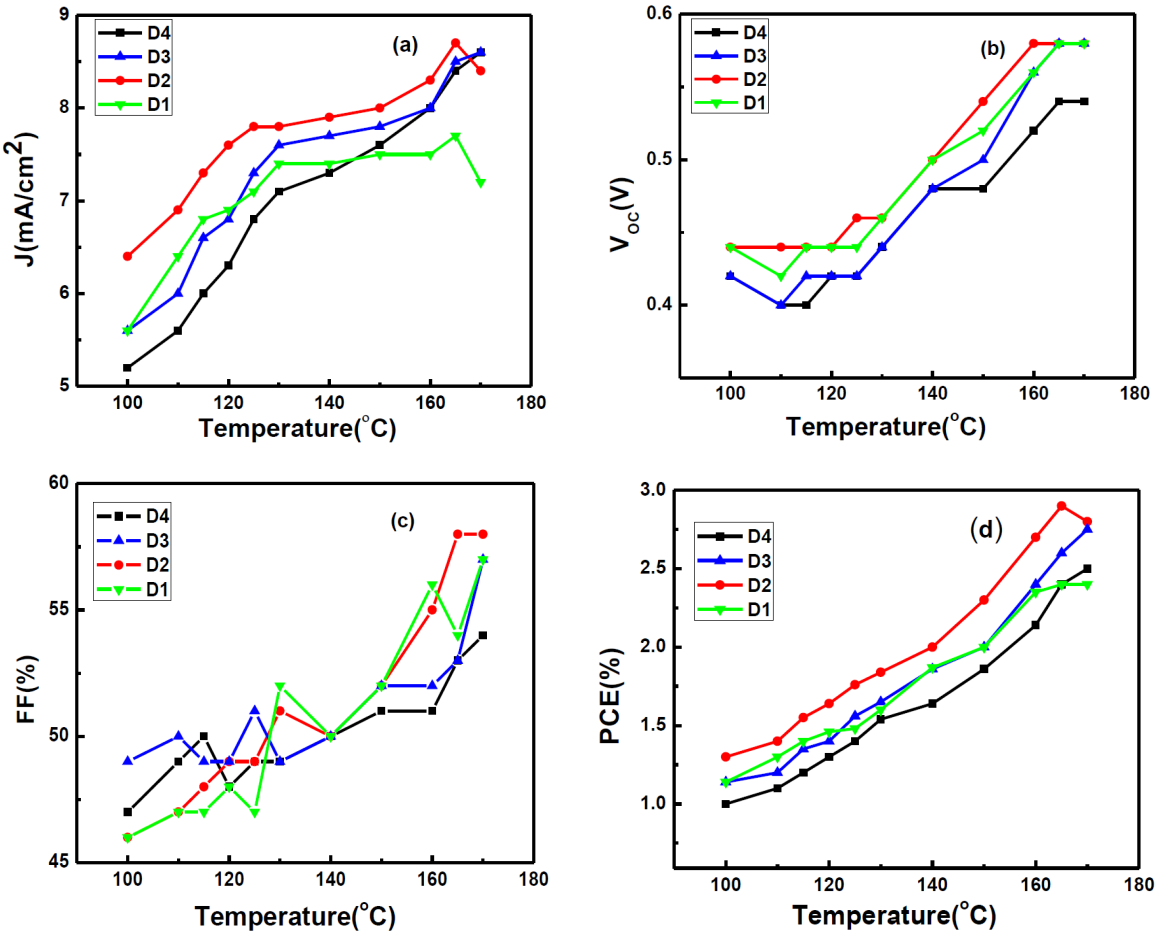

Figure 4. Effect of annealing temperature on various OPV parameters of the devices with different thicknesses having Al as top electrode: Dependence of (a) J_{SC}, (b) V_{OC}, (c) FF and (d) PCE on annealing temperature.

To address the optimization of top-electrode effect on OPVs, a thin layer of LiF and Ca were deposited between Al and organic-active layer in the fabricated bulk heterojunction polymeric solar cells as shown in Figure 1b. The insertion of these thin layers significantly enhances the fill factor and stabilizes the open-circuit voltage of the OPVs.

Current-density-voltage characteristics of the OPVs with different metal electrodes at optimized annealing temperature of 130 °C are shown in Figure 5. The parameters of the device with thin layer of LiF and Ca enhance when compared to a device with just Al thin layer. This may be due to either orientation of the LiF/Ca or doping of the device active layer. At this optimum value of annealing temperature and 120-nm thickness, devices' fill factor was enhanced with consistent open-circuit voltage as shown in Figure 6. The organic solar cell with Ca based electrode performed extremely well at lower annealing temperature and obtained power-conversion efficiency of 2.78%. All the

device parameters, such as J_{SC}, V_{OC} and FF, were improved at optimum annealing temperature of 130 °C.

The summary of all devices parameters is reported in Table 2. The high performance is due to the high fill factor, low series resistance of 9.54 ohms and good diode behavior with high rectification.

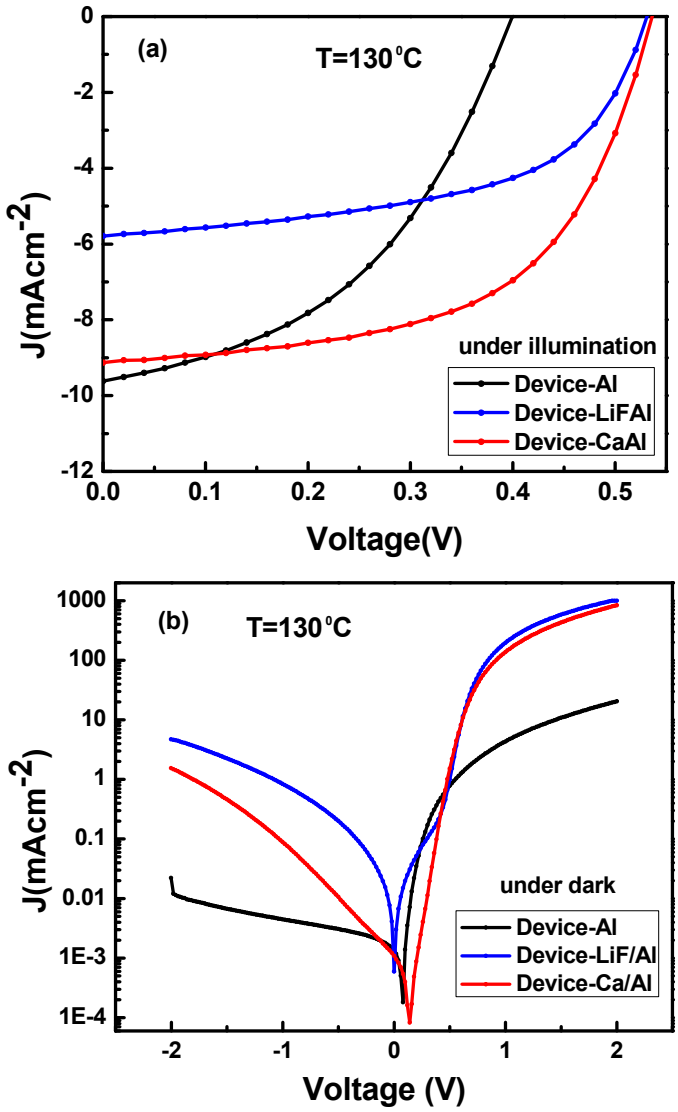

Figure 5. J-V characteristics of the spin coating devices with different metal contacts at optimum annealing temperature of 130 °C under (a) Illumination and (b) dark.

Table 2. Summary of OPVs parameters of devices at three different top electrodes at optimum thermal annealing of 130 °C.

Devices	J_{sc} (mA/cm^2)	V_{oc} (V)	FF (%)	PCE (%)
Al-electrode	9.6	0.40	44	1.71
LiF/Al-electrode	5.8	0.54	54	1.70
Ca/Al-electrode	9.1	0.54	56	2.78

The thermal annealing effect was observed by plotting devices parameters with respect to annealing temperature for the three devices as shown in Figure 6.

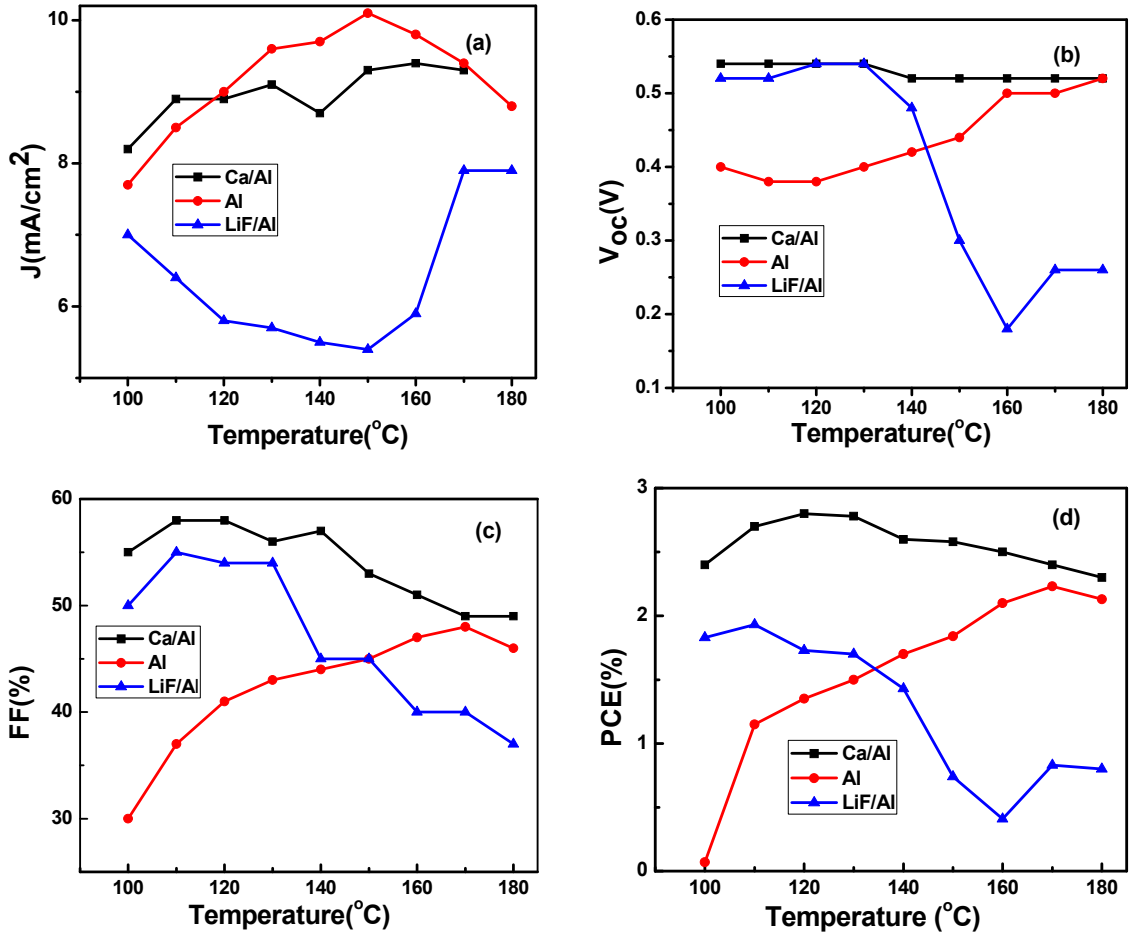

Figure 6. Effect of thermal annealing on various OPV parameters of the devices with different metal contacts: Dependence of (a) J_{SC}, (b) V_{OC}, (c) FF and (d) PCE on annealing temperature at optimum thickness of 120 nm.

The increasing trend in overall devices parameters is observed at certain optimum value of annealing temperature. Moreover, increasing the annealing temperature above a certain limit, Al-based device performs better and is consistent with value reported in literature. Whereas the efficiency of both LiF- and Ca-based OPVs decreases with rising annealing temperature, probably due to formation of oxides layer at semiconductor-metal interface. Thermal annealing above 130 °C causes oxide layer. This metal-oxide layer is electrically insulating, increases series resistance and creates a transport barrier, eventually degrading the performance of the device as reported in refs [36,37]. Thermal annealing at high temperature increases V_{oc} values of Al device and does not seriously affect V_{oc} values of Ca/Al device probably, the former is less reactive/sensitive to oxygen than the latter at high temperature. Nevertheless, it is not the only reason of bad performance. The performance of these devices could be further improved by optimizing parameters such as the film roughness (morphology), film thickness, decreasing oxidation, solvent selection, blending ratio and the use of other post-growth treatments [39,40,41].

4. Conclusions

We investigated optimum parameters of organic solar cell devices, such as active-layer thickness, annealing temperature, and the role of interlayers before Al deposition. Device D2 with 120 nm active-layer thickness performed well at 10 minutes thermal annealing of 165 °C, resulting in maximum power-conversion efficiency of 2.9%. Organic solar cells with Ca-based Al contact performed relatively better at lower annealing temperature, and started degrading when the temperature increased above 130 °C, PCE reached to 2.78% unlike in the case of LiF/Al and Al where it is just 1.7% and 1.71% respectively. In fact, this is owing to their proper energy-level alignment with active materials which facilitates exciton diffusion/dissociation and charge collection to their respective electrodes. Therefore, thermal annealing has a significant role on the overall performance of the devices. In summary, with optimum parameters the performance of polymeric solar cells can be improved but the issue of stability of such devices is yet to be addressed.

Acknowledgement

The author thanks the Higher Education Commission (HEC) of Pakistan for sponsoring the research Project No: PM-IPFP/HRD/HEC/2012/4021.

Conflict of Interest

The authors declare that there is no conflict of interest regarding the publication of this manuscript.

References

1. Yu G, Gao J, Hummelen JC, et al. (1995) Polymer photovoltiac cells: Enhanced efficiencies via a network of internal donor-acceptor heterojunctions. *Science* 270: 1789.
2. Halls J, Walsh C, Greenham N, et al. (1995) Efficient photodiodes from interpenetrating polymer networks. *Nature* 376: 498.
3. Ma W, Yang C, Gong X, et al. (2005) Thermally stable, efficient polymer solar cells with nanoscale control of the interpenetrating network morphology. *Adv Funct Mater* 15: 1617–1622.
4. Dennler G, Scharber MC, Brabec CJ (2009) Polymer-Fullerene bulk-heterojunction solar cells. *Adv Mater* 21: 1323–1338.
5. Xie Y, Zabihi F, Eslamian M (2016) Fabrication of highly reproducible polymer solar cells using ultrasonic substrate vibration posttreatment. *J Photon Energy* 6: 045502–045502.
6. Zabihi F, Chen Q, Xie Y, et al. (2016) Fabrication of efficient graphene-doped polymer/fullerene bilayer organic solar cells in air using spin coating followed by ultrasonic vibration post treatment. *Superlattice Microst* 100: 1177–1192.
7. Anderson TE, Köse ME (2016) Impact of solution casting temperature on power conversion efficiencies of bulk heterojunction organic solar cells. *J Photoch Photobio A* 318: 51–55.
8. Oklobia O, Shafai T (2013) A quantitative study of the formation of PCBM clusters upon thermal annealing of P3HT/PCBM bulk heterojunction solar cell. *Sol Energ Mat Sol C* 117: 1–8.

9. Vanlaeke P, Swinnen A, Haeldermans I, et al. (2006) P3HT/PCBM bulk heterojunction solar cells: Relation between morphology and electro-optical characteristics. *Sol Energ Mat Sol C* 90: 2150–2158.
10. Oklobia O, Shafai T (2013) A study of donor/acceptor interfaces in a blend of P3HT/PCBM solar cell: Effects of annealing and PCBM loading on optical and electrical properties. *Solid State Electron* 87: 64–68.
11. Wang Q, Xie Y, Soltani-Kordshuli F, et al. (2016) Progress in emerging solution-processed thin film solar cells—Part I: polymer solar cells. *Renew Sustain Ener Rev* 56: 347–361.
12. Reyes-Reyes M, Kim K, Carroll DL (2005) High-efficiency photovoltaic devices based on annealed poly(3-hexylthiophene) and 1-(3-methoxycarbonyl)-propyl-1-phenyl-(6,6)C_{61} blends. *Appl Phys Lett* 87: 083506.
13. Reyes-Reyes M, Kim K, Dewald J, et al. (2005) Meso-structure formation for enhanced organic photovoltaic cells. *Org Lett* 7: 5749–5752.
14. Li G, Shrotriya V, Huang J, et al. (2005) High-efficiency solution processable polymer photovoltaic cells by self-organization of polymer blends. *Nat Mater* 4: 864–868.
15. Service R (2011) Solar energy. Outlook brightens for plastic solar cells. *Science* 332: 293.
16. Li G, Shrotriya V, Yao Y, et al. (2005) Investigation of annealing effects and film thickness dependence of polymer solar cells based on poly(3-hexylthiophene). *J Appl Phys* 98: 043704.
17. Moulé AJ, Bonekamp JB, Meerholz K (2006) The effect of active layer thickness and composition on the performance of bulk-heterojunction solar cells. *J Appl Phys* 100: 094503.
18. Nam YM, Huh J, Jo WH (2010) Optimization of thickness and morphology of active layer for high performance of bulk-heterojunction organic solar cells. *Sol Energ Mat Sol C* 94: 1118–1124.
19. Kirchartz T, Agostinelli T, Campoy-Quiles M, et al. (2012) Understanding the thickness-dependent performance of organic bulk heterojunction solar cells: the influence of mobility, lifetime, and space charge. *J Phys Chem Lett* 3: 3470–3475.
20. Rim SB, Fink RF, Schöneboom JC, et al. (2007) Effect of molecular packing on the exciton diffusion length in organic solar cells. *Appl Phys Lett* 91: 173504.
21. O'Connor B, An KH, Pipe KP, et al. (2006) Enhanced optical field intensity distribution in organic photovoltaic devices using external coatings. *Appl Phys Lett* 89: 233502.
22. Breyer C, Vogel M, Mohr M, et al. (2006) Influence of exciton distribution on external quantum efficiency in bilayer organic solar cells. *Phys Status Solidi B* 243: 3176–3180.
23. Chang CC, Lin CF, Chiou JM, et al. (2010) Effects of cathode buffer layers on the efficiency of bulk-heterojunction solar cells. *Appl Phys Lett* 96: 263506.
24. Vogel M, Doka S, Breyer C, et al. (2006) On the function of a bathocuproine buffer layer in organic photovoltaic cells. *Appl Phys Lett* 89: 163501.
25. Jiang X, Xu H, Yang L, et al. (2009) Effect of CsF interlayer on the performance of polymer bulk heterojunction solar cells. *Sol Energ Mat Sol C* 93: 650–653.
26. Wang Y, Yang L, Yao C, et al. (2011) Enhanced performance and stability in polymer photovoltaic cells using lithium benzoate as cathode interfacial layer. *Sol Energ Mat Sol C* 95: 1243–1247.
27. Abachi T, Cattin L, Louarn G, et al. (2013) Highly flexible, conductive and transparent MoO_3/Ag/MoO_3 multilayer electrode for organic photovoltaic cells. *Thin Solid Films* 545: 438–444.

28. Zhao SH, Chang JK, Fang JJ, et al. (2013) Efficiency enhancement caused by using LiF to change electronic structures in polymer photovoltaics. *Thin Solid Films* 545: 361–364.
29. Brabec CJ, Shaheen SE, Winder C, et al. (2002) Effect of LiF/metal electrodes on the performance of plastic solar cells. *Appl Phys Lett* 80: 1288–1290.
30. Zhao C, Qiao X, Chen B, et al. (2013) Thermal annealing effect on internal electrical polarization in organic solar cells. *Org Electron* 14: 2192–2197.
31. Yazawa K, Inoue Y, Yamamoto T, et al. (2006) Twist glass transition in regioregulated poly(3-alkylthiophene). *Phys Rev B* 74: 094204.
32. Kim K, Liu J, Namboothiry MA, et al. (2007) Roles of donor and acceptor nanodomains in 6% efficient thermally annealed polymer photovoltaics. *Appl Phys Lett* 90: 163511.
33. Sariciftci NS, Smilowitz L, Heeger AJ, et al. (1992) Photoinduced electron transfer from a conducting polymer to buckminsterfullerene. *Science* 258: 1474–1476.
34. Brabec CJ, Gowrisanker S, Halls JJ, et al. (2010) Polymer-fullerene bulk-heterojunction solar cells. *Adv Mater* 22: 3839–3856.
35. Park SH, Roy A, Beaupré S, et al. (2009) Bulk heterojunction solar cells with internal quantum efficiency approaching 100%. *Nat Photonics* 3: 297–302.
36. Shah SK, Abbas M, Ali M, et al. (2013) Optimal construction parameters of electrosprayed trilayer organic photovoltaic devices. *J Phys D Appl Phys* 47: 045106.
37. Ali M, Abbas M, Shah SK, et al. (2012) Realization of solution processed multi-layer bulk heterojunction organic solar cells by electro-spray deposition. *Org Electron* 13: 2130–2137.
38. Pope M, Swenberg CE (1999) *Electronic processes in organic crystals and polymers*, Oxford University Press on Demand.
39. Bertho S, Janssen G, Cleij TJ, et al. (2008) Effect of temperature on the morphological and photovoltaic stability of bulk heterojunction polymer: fullerene solar cells. *Sol Energ Mat Sol C* 92: 753–760.
40. Jørgensen M, Norrman K, Gevorgyan SA, et al. (2012) Stability of polymer solar cells. *Adv Mater* 24: 580–612.
41. Hong J, Kim YJ, Kim YH, et al. (2016) Thermally Stable Dibenzo[def,mno]chrysene-Based Polymer Solar Cells: Effect of Thermal Annealing on the Morphology and Photovoltaic Performances. *Macromol Chem Phys* 217: 2116–2124.

AIMS Press